MODELLING TRANSITION USING AN INTERMITTENCY TRANSPORT EQUATION

K. Lodefier, B. Merci, C. De Langhe and E. Dick
Dept. of Flow, Heat and Combustion Mechanics,
Ghent University,
St. Pietersnieuwstraat 41, B-9000 Gent, Belgium
koen.lodefier@rug.ac.be

ABSTRACT

A transition model for describing bypass transition is presented. It is based on a two-equations $k-\omega$ model and a dynamic equation for intermittency factor. The intermittency factor is a multiplier of the turbulent viscosity computed by the turbulence model.The quality of the transition model, developed on flat plate test cases, is illustrated for cascades.

INTRODUCTION

In gas turbine engines, laminar-turbulent transition occurs in bypass mode. This means that transition is induced by pressure coupling between the freestream and a laminar boundary layer. Turbulence models that can be used in regions with low turbulence level are basically able to describe this form of transition. However, in general, the transition is detected too early and the transition phase is too short (Savill, 1992). Improvement of the simulation of the transition can be obtained by combining a turbulence model with a description of the intermittency, i.e. the fraction of time the flow is turbulent during the transition phase. By letting the intermittency grow from zero to unity, start and evolution of transition can be imposed.

CHOICE BETWEEN $K-\varepsilon$ AND $K-\omega$

The concept of a dynamic intermittency equation can be applied to any type of two-equations turbulence model. The choice between a $k-\omega$ and a $k-\varepsilon$ model has to be made. To illustrate the difference in behaviour between a $k-\varepsilon$ model and a $k-\omega$ model, we use the low-Re Yang-Shih model (Yang, 1993) and the high-Re SST model (Menter, 1994). Note that, in order to describe near wall behaviour, the low-Re extension of a $k-\varepsilon$ model is needed. This is not necessary for a $k-\omega$ model. Already in high-Re formulation, a $k-\omega$ model allows calculation in the near wall region. The low-Re modifications of a $k-\omega$ model improve the asymptotic behaviour near the wall and the transition behaviour of the model (Wilcox, 1994). Since, here, we aim at modelling transition with a supplementary intermittency equation, we do not use the low-Re modifications meant for transition.

We take as test case the T3A flat plate flow from ERCOFTAC (http://cfd.me.umist.ac.uk/ercoftac/) with turbulence intensity $Tu = 3\%$ in the oncoming flow. Figure 1 shows the variation of the friction coefficient for the T3A flow obtained with the $k-\varepsilon$ and $k-\omega$ models, when used without modifications. The models predict start of transition far before the physical transition which takes place at approximately $Re_x = 1.5e5$. This deficiency of turbulence models without modification is well known (Savill, 1992).

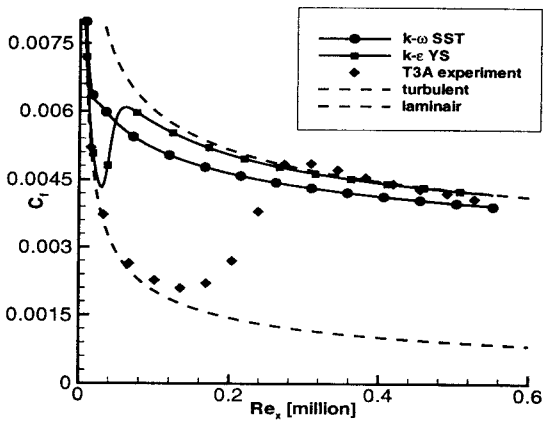

Figure 1: T3A SKIN FRICTION EVOLUTION FOR ORIGINAL k-ε AND k-ω MODELS.

Figure 2 shows the variation of the friction coefficient for the same test case when the production terms are suppressed up to $Re_x = 2.0e5$ and when they are switched fully on at this location. The chosen switch location is well after the physical transition location. This result illustrates the explosive character of the transitional behaviour of turbulence models used without modification. The basic reason for the explosive character is that the turbulence models are forced to work on laminar velocity profiles. Turbulence models have been calibrated for turbulent flows only, and their behaviour on laminar flows has not been considered during design. Some consequences are illustrated in figure 3.

Figure 3a shows profiles for the turbulent viscosity obtained for the T3A flow, when the $k-\varepsilon$ model with the full production term is applied to a laminar flow field. In other words, the turbulent viscosity is set to zero in the Navier-Stokes equations. A comparison is made with the turbulent viscosity, obtained with the same model, in turbulent flows. The turbulent flow is obtained by allowing the turbulent viscosity in the Navier-Stokes equations. The corresponding C_f behaviour for the turbulent flows was already shown in Figure 1. From Figure 3a it is clear that the $k-\varepsilon$ model results in excessive values of the turbulent viscosity, when it is applied to a laminar flow. The corresponding values of the $k-\omega$ model, shown in Figure 3b, are much lower. The behaviour of the $k-\omega$ model is better than the behaviour of the $k-\varepsilon$ model since it does not rely on near-wall functions, which have been tuned on turbulent velocity fields.

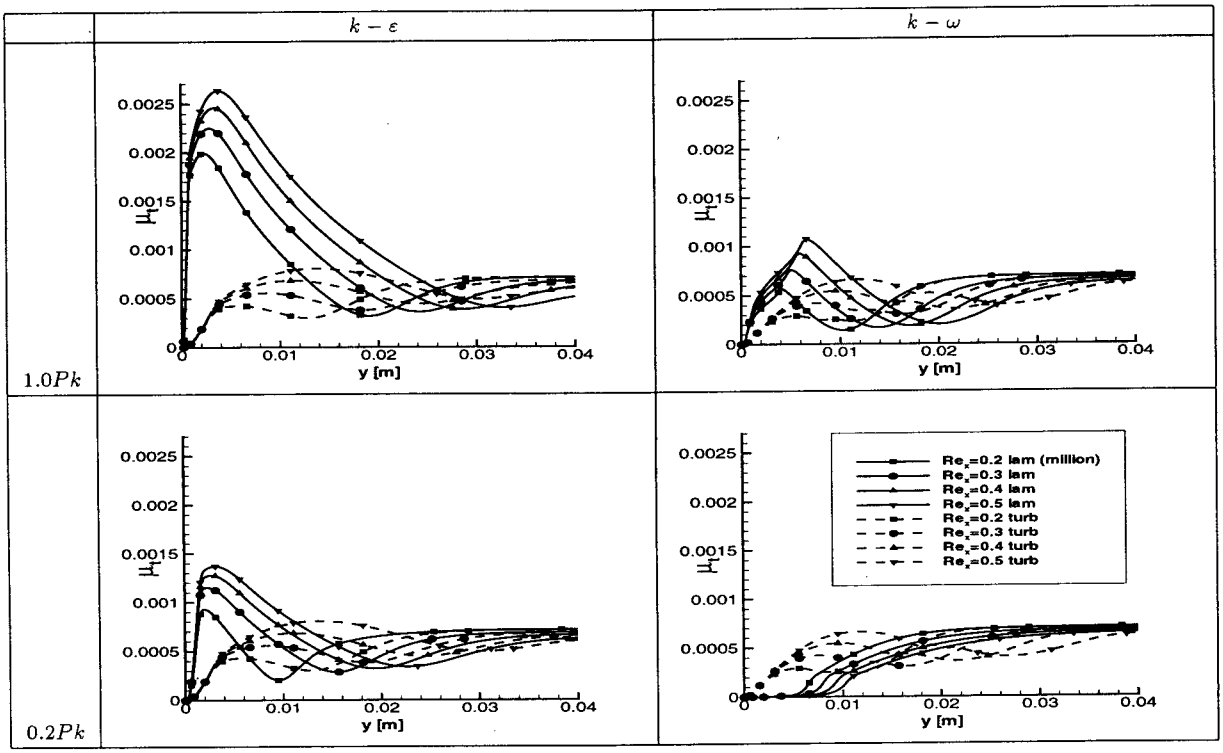

Figure 3: μ_t PROFILES AT DIFFERENT Re_x LOCATIONS ON LAMINAR AND TURBULENT VELOCITY PROFILES.

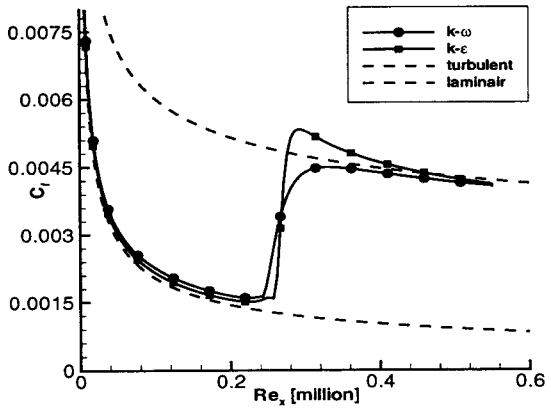

Figure 2: T3A SKIN FRICTION EVOLUTION FOR k-ε AND k-ω MODELS WITH SUPPRESSION OF TURBULENCE UNTIL $Re_x = 0.2e6$.

The incorrect behaviour of turbulence models applied to laminar flows illustrates that, in order to correctly describe intermittent flows during transition, a distinction has to be made between the turbulent parts and the non-turbulent parts of the flow. The turbulence model then only acts on the turbulent parts. Making the distinction between the two parts in the flow requires conditional averaging of the Navier-Stokes equations, as done by Steelant and Dick (1996). This doubles the number of equations in the description of the flow. A conditional averaging technique is seen as too complex for industrial applications. It is not compatible with commercial CFD software and the computing time practically doubles.

The consequence of the foregoing observations is that with globally averaged Navier-Stokes equations, the behaviour of a turbulence model in the pre-transition zone is principally incorrect. In order to bring the behaviour closer to reality, turbulence has to be damped. A $k-\omega$ model and a $k-\varepsilon$ model react differently to damping of the production terms Figures 3c and 3d show the turbulent viscosity obtained by multiplying the production terms with 0.2. The reduction obtained in turbulent viscosity is not substantial for the $k-\varepsilon$ model. For the $k-\omega$ model, turbulent viscosity becomes very small close to the wall.

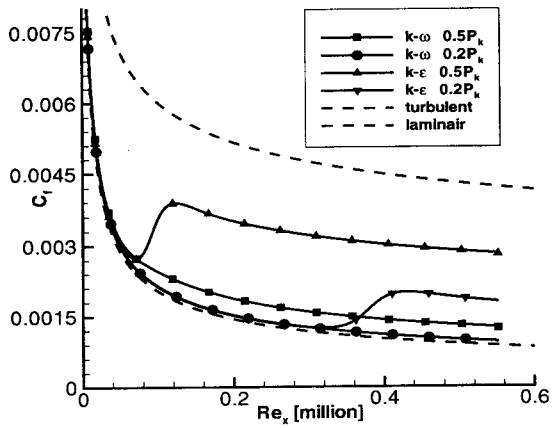

Figure 4: T3A SKIN FRICTION EVOLUTION FOR k-ε AND k-ω MODELS WITH REDUCED PRODUCTION TERMS.

In order to further illustrate the difference in behaviour of both models, Figure 4 shows the obtained skin friction co-

efficient when the production terms in the turbulence model have been multiplied with a factor 0.2 and 0.5. Also the turbulent viscosity used in the Navier-Stokes equations has been multiplied by this factor. The more explosive character of the $k-\varepsilon$ model is clear. This comparison shows again that by steering the production term, a $k-\omega$ model can be easier controlled than a $k-\varepsilon$ model. For this reason we give here preference to the $k-\omega$ model. We use the SST model (Menter, 1994).

EQUATION FOR INTERMITTENCY FACTOR

The intermittency equation is a convection-diffusion equation with a source term, as developed by Steelant and Dick (1996):

$$\frac{\partial(\rho\gamma)}{\partial t}+\frac{\partial(\rho U_i\gamma)}{\partial x_i}=2F_sP_{\gamma,SD}+\frac{\partial}{\partial x_i}\left[(\mu+\frac{\mu_t}{\sigma_\gamma})\frac{\partial\gamma}{\partial x_i}\right], \quad (1)$$

with $\sigma_\gamma = 1.0$. The role of the diffusion term is to allow a gradual variation of γ towards zero in the freestream. The boundary condition for γ at the wall is zero normal derivative (inviscid boundary condition).

For zero-pressure-gradient, the intermittency γ can be described algebraically according to Dhawan and Narasimha (1958). From this relation, the production term for intermittency was developed by Steelant and Dick (2001). It contains a factor which accounts for the turbulent spot growth and which depends on the turbulence intensity at the start of transition, on a local acceleration parameter and on the freestream velocity. Furthermore, it contains a factor which takes into account the distributed breakdown of the turbulent spots. This is necessary, since the Dhawan-Narasimha law is only completely valid for natural transition. In this type of transition, spots appear in a very narrow region in the boundary layer. In bypass transition, spots appear in a much more extended region. This is called distributed breakdown. As a consequence, the intermittency factor does not follow the Dhawan-Narasimha law for small values of γ and the mentioned factor corrects for this effect. The production $P_{\gamma,SD}$ is used here as it has been developed by Steelant and Dick (2001), but with the original compressibility correction of Boyle and Simon (1999).

Here, a new factor, F_s, is introduced in the production term in Eq. (1). It is a starting function inspired by the function used by Menter et al. (2002). F_s is zero before start of transition, and rapidly goes to unity after the onset point. The complete expression Eq. (5) is based on different factors, as explained hereafter.

Firstly, the value of Re_θ at start of transition is determined. The correlation proposed by Mayle (1991) is used:

$$Re_{\theta t}=420Tu^{-0.69} \quad (2)$$

Eq. (2), is based on flat plate experiments where Tu is the turbulence intensity at the leading edge. For the flat plate test cases, we use this turbulence intensity. For cascades, the turbulence intensity at the leading edge of the profile does not characterize the turbulence affecting the transition zone. We replace it by the turbulence intensity at the boundary layer edge in the zone before the start of transition. It turns out that this turbulence intensity is nearly constant for the suction side of a cascade profile. As a consequence, this turbulence intensity, obtained from the Navier-Stokes equations, is determined with high confidence. At the pressure side, turbulence intensity varies rapidly. The value, however, is very large (typically around 15%). Eq. (2) then produces small values of Re_θ, not sensitive to the precise value of Tu.

Secondly, following a suggestion by Menter et al. (2002), the non-dimensional group $\frac{Sy^2}{\nu}$ is used to estimate Re_θ. To analyze this non-dimensional group, we use the Pohlhausen self-similarity boundary layer velocity profile representation. The non-dimensional group is zero at the wall and at the edge of the boundary layer, with a single maximum value somewhere midway the boundary layer. This maximum value equals $2.2Re_\theta$. Therefore, $\frac{Sy^2}{2.2\nu}$ is used as an indicator of Re_θ, and the transition is imposed when $\frac{Sy^2}{2.2\nu}$ reaches the critical $Re_{\theta t}$ resulting from the Mayle criterion.

With Eq. (2), the factor ξ, given by:

$$\xi = \frac{1}{Re_{\theta t}}\frac{Sy^2}{2.2\nu} \quad (3)$$

is lower than 1 before start of transition and reaches unity in one point along the line perpendicular to the wall at the station where transition occurs. With the factor ξ, start of transition is calculated using only local variables: shear rate S and distance to the wall y. However, in the Mayle correlation, Eq. (2), start of transition is determined on the basis of the Dhawan-Narasimha law. As already mentioned, in by-pass transition there is distributed breakdown, so that the start of transition should be advanced. To that purpose, a factor 1.12 is introduced in Eq. (5). This factor has been determined by numerical optimization. Finally, it is noted that the factor $\frac{Sy^2}{\nu}$ becomes large far from the wall. This may cause non-physical intermittency in the freestream. A limiter on the distance to the wall y is therefore applied outside the boundary layer.

The term in Eq. (5), added to 1.12ξ, has as objective to maintain the transition detector above unity after the start of transition. The term grows with γ and μ_t. Its form is not critical. The factor 'a' detects the presence of the boundary:

$$a=min(1;20b^4) \quad , \quad b=\frac{U^2}{\nu\ max(S;0.0001)10^5} \quad (4)$$

Due to the high strain rate in the boundary layer, $20b^4$ is very small. Outside the boundary layer, the strain rate becomes small. The factor 'a' thus switches very rapidly from a low value ($\cong 0$) to 1 outside the boundary layer. Using the factor $(1-a)$ in Eq. (5) prevents that transition is switched on in the freestream.

It is numerically observed that the factor F_s has to be amplified (but bound to unity) in order to activate the production term in Eq. (1) sufficiently rapidly. To that purpose, a factor 20 (which is again not critical) is introduced in the final expression:

$$F_s=\min\left[20\max\left(1.12\xi+0.1(1-a)\frac{\gamma\mu_t}{\mu}-1;0\right);1\right] \quad (5)$$

Finally, it is noted that the parameter ξ from Eq. (3) has a profile in the boundary layer, so that the start of transition and the γ profile are not constant perpendicular to the wall. This results in an important underevaluation of the intermittency γ close to the wall. Therefore, to compensate for the lower γ values close to the wall, the source term for intermittency is multiplied by the factor 2 in Eq. (1). In regions away from the wall, the diffusion term compensates for excessive values of γ due to this factor. The multiplier 2 has been obtained by numerical optimization on a number of flat plate test cases (see later).

START OF TRANSITION WITH SST MODEL

For both the k and ω equations, the production part of the source term is multiplied by a function of γ and a (with a the boundary layer detector of Eq. (4)). Before transition and inside the boundary layer ($\gamma = 0$ and $a = 0$), the production term is multiplied by $\frac{\mu}{\mu_t}$. Consequently, the turbulence model is started up early but excessive creation of turbulent features is avoided. As a result, at start of transition, turbulent properties have a non-zero value. Small, but non-zero starting values are essential to let grow turbulent properties sufficiently fast in the transition zone. Outside the boundary layer or after transition, the full production terms are used. Incorporating these considerations yields:

$$[a + (1 - a)[\gamma + (1 - \gamma)\max(\frac{\mu}{\mu_t}; 0.1)]]P_{k/\omega} \qquad (6)$$

The factor 0.1 is introduced in order to ensure sufficient production throughout the domain.

The dissipation part in the transport equations for k and ω is left unaltered in the complete domain.

NUMERICAL METHOD AND TEST CASES

All calculations have been done with the package Fluent, using its steady solver. The built-in turbulence models have been disabled. Instead, self written equations for k, ω and γ have been implemented via user defined functions.

For development and testing of the model, bypass transitional flows on adiabatic flat plates with sharp leading edges, proposed by Kuan and Wang (1990) (KW-case) and by ERCOFTAC (T3-cases) (http://cfd.me.umist.ac.uk/ercoftac/) have been used. Three test cases with zero-pressure-gradient were considered (KW, T3A and T3B), and three test cases with pressure distribution (T3C1, T3C2 and T3C5). The pressure distributions are typical for the aft part of the suction side of low pressure turbines. The specifications of the different flat plate test cases are given in Table 1, where U_i stands for the oncoming velocity and Tu_{le} for the turbulence intensity in the leading edge plane. The experimental decay of freestream turbulence has been reproduced in the calculations by setting the inflow value of ω. Values for k and ω in the leading edge plane are listed in Table 1.

The quality of the model, developed on the basis of the flat plate test cases, is illustrated for two cascade test cases of the Von Karman Institute (VKI), measured at the University of Genova (http://transition.imse.unige.it/cases/goa). Reynolds number based on the chord and exit velocity for VKI1 is $Re_{2c} = 1.6e6$ and for VKI2 $Re_{2c} = 5.9e5$. The specifications of the VKI test cases are given in Table 2, in the same form as for the flat plate test cases. Further, the model has been applied to cascade test cases with heat transfer, measured by Arts and Lambert de Rouvroit (1990). The considered test cases are MUR239 and MUR241, with 6% of turbulence intensity in the oncoming flow. For reasons of explanation, also data are used of the test cases MUR247 and MUR116. These cases have low turbulence intensity in the oncoming flow. The specifications of the MUR test cases are given in Table 2. The incoming turbulence level Tu_i is measured 55 mm upstream of the leading edge. Also the exit isentropically determined Mach number and the exit Reynolds number based on the chord are specified.

For all flat plate test cases the first grid point is located such that $y^+ < 1$. A stretching factor has been applied perpendicular to the wall. In stream-wise direction, also a stretching factor has been applied near the leading edge. For the pressure gradient test cases, a curved wall (with

Table 1: DESCRIPTION OF FLAT PLATE TEST CASES.

Case	$U_i(m/s)$	$Tu_{le}(\%)$	$k_{le}(m^2/s^2)$	$\omega_{le}(s^{-1})$
KW	13.8	1.1	0.035	167
T3A	5.4	3	0.042	232
T3B	9.4	6.14	0.488	315
T3C1	6.12	7.78	0.324	430
T3C2	5.3	3	0.0313	254
T3C5	9.26	3	0.103	500

Table 2: DESCRIPTION OF CASCADE TEST CASES.

Case	$U_i(m/s)$	$Tu_{le}(\%)$	$k_{le}(m^2/s^2)$	$\omega_{le}(s^{-1})$
VKI1	28.1	2	3	1300
VKI2	10.5	3.25	1.05	475

Case	$M_{2,is}$	$Tu_i(\%)$	$Re_{c,2}$
MUR239	0.922	6	2.10^6
MUR247	0.922	1	2.10^6
MUR241	1.089	6	2.10^6
MUR116	1.090	0.8	2.10^6

inviscid boundary conditions) has been placed opposite the flat plate, to get the appropriate velocity distribution. The inlet is 200 mm upstream of the leading edge.

For the cascade test cases, the grid point nearest to the wall obeys $y^+ < 1$. A turbulent time scale bound has been applied according to Medic and Durbin (2002), in order to suppress excessive generation of turbulent kinetic energy at the leading edge:

$$T = min\left[\frac{1}{C_\mu \omega}, \frac{0.6}{\sqrt{6}C_\mu |S|}\right]$$

The turbulent viscosity is calculated by $\mu_t = C_\mu \rho k T$.

NUMERICAL RESULTS: FLAT PLATE TEST CASES

Figure 5 shows the skin friction evolution for the flat plate test cases. The correspondence with the experiments generally is very good except for the T3C2 case. The T3C cases all have an acceleration phase followed by a deceleration phase. For the T3C1 and T3C5 cases, transition occurs during the acceleration. For the T3C2 case, the acceleration is very long and transition occurs at the beginning of the deceleration phase. The Mayle-criterion predicts the transition too early for such a flow. The flat plate test cases have been used to determine some of the expressions in the transition model and to tune some of the parameters. The two most essential parameters in the current model are the multiplier 2 in the production term in Eq. (1) and the multiplier 1.12 in F_s (Eq. (5)). Alle other terms are basically not critical.

NUMERICAL RESULTS: CASCADE TEST CASES

For the cascade test cases, no further tuning of the transition model has been done. There are, however, two essential differences with respect to the flat plate test cases. Firstly, the turbulence intensity level introduced into the Mayle correlation is now the turbulence intensity at the edge of the boundary layer before start of transition. Secondly, for cascades, the self-similarity condition for Pohlhausen representation is not fulfilled. This results in $(\frac{Sy^2}{2.2\nu})_{max}$ values which are much lower than Re_θ. Re_θ is not only locally determined but it results also from previous history. We found

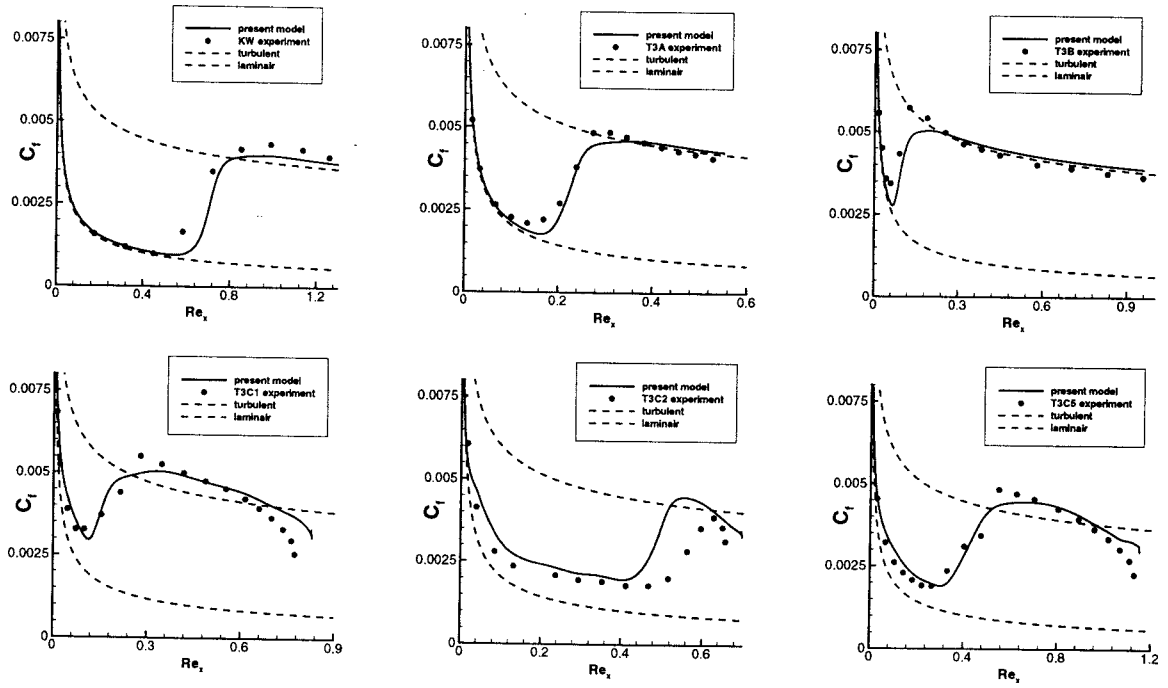

Figure 5: SKIN FRICTION EVOLUTION FOR THE FLAT PLATE TEST CASES.

from numerical experiments that, for strongly accelerating flows, the ratio between Re_θ and the non-dimensional group is near to two. Therefore, the factor ξ (Eq. 3) is multiplied by 1.8. This factor is the average ratio observed in the calculations.

Figure 6 shows the calculated skin friction and intermittency profiles for the VKI test cases. The turbulence intensity at the start of transition has been used in the Mayle correlation. This means 1.2% for VKI1 and 1.5% for VKI2 on the suction side. For both cases there is no transition on the pressure side. On the suction side, the start of transition is well represented. Only for the VKI1 test case, the skin friction peak after transition is not as high as in the experiments.

Figure 7 shows the calculated surface heat transfer coefficient and intermittency profiles for the MUR239 and MUR 241 (Tu_i = 6%) test cases. The effect of freestream turbulence level on the heat transfer in the laminar boundary layer has been incorporated in the turbulent viscosity, as proposed by Smith and Kuethe (1966):

$$\mu_{t,lam} = 0.164 Tu U_\infty y$$

The distance from the wall 'y' has again been limited outside the boundary layer. The turbulence intensity at start of transition is used in the Mayle correlation. This means 1.5% for the suction side and 15% for the pressure side for MUR239 and 1.6% and 15% for MUR241. The low turbulence level experiments MUR247 (Tu_i = 1%) and MUR116 (Tu_i = 0.8%) have been added in order to show what the results might be for much lower turbulence level (in analogy with the theoretical laminar C_f profiles in fig. 1).

The results for the suction side are relatively good. The transition is detected at the correct position. The transition region also has the correct length. The heat transfer level after transition is too low. This is a deficiency of the turbulence model. Also a fully turbulent calculation (not shown) leads to the same underprediction of the heat transfer in the turbulent zone of the boundary layer. The predicted heat transfer coefficient in the laminar part is in good agreement with the expriments. This is due to the supplementary viscosity $\mu_{t,lam}$ by the Smith and Kuethe formula. At the pressure side, the transition is detected somewhat too late. In reality, transition occurs almost immediately after the leading edge. This late transition happens despite the very low value of Re_θ obtained from the Mayle criterion ($\sim$ 65).

CONCLUSIONS

A transition model, based on a dynamic transport equation for the intermittency factor, in combination with the SST turbulence model, has been presented. The choice of a $k-\omega$ type turbulence model has been explained.

The quality of the model, developed on the basis of flat plate test cases, has been illustrated on cascades without further tuning. Skin friction profiles and heat transfer coefficient profiles have been presented.

ACKNOWLEDGMENTS

The work reported in this paper was performed within the research project UTAT-'Unsteady Transitional Flows in Axial Turbomachines', funded by the European Commission GROWTH programme under contract number G4RD-CT-2001-00628. The second author works as Postdoctoral Fellow of the Fund for Sientific Research - Flanders (Belgium).

REFERENCES

Arts, T., and Lambert de Rouvroit, M., Aero-thermal investigation of a highly loaded transonic linear turbine guide vane cascade. technical note 174, von Karman Institute, 1990.

Boyle, B. J., and Simon, F. F., Mach number effects on turbine blade transition length prediction. *J. of Turbomachinery*, 121:694–702, 1999.

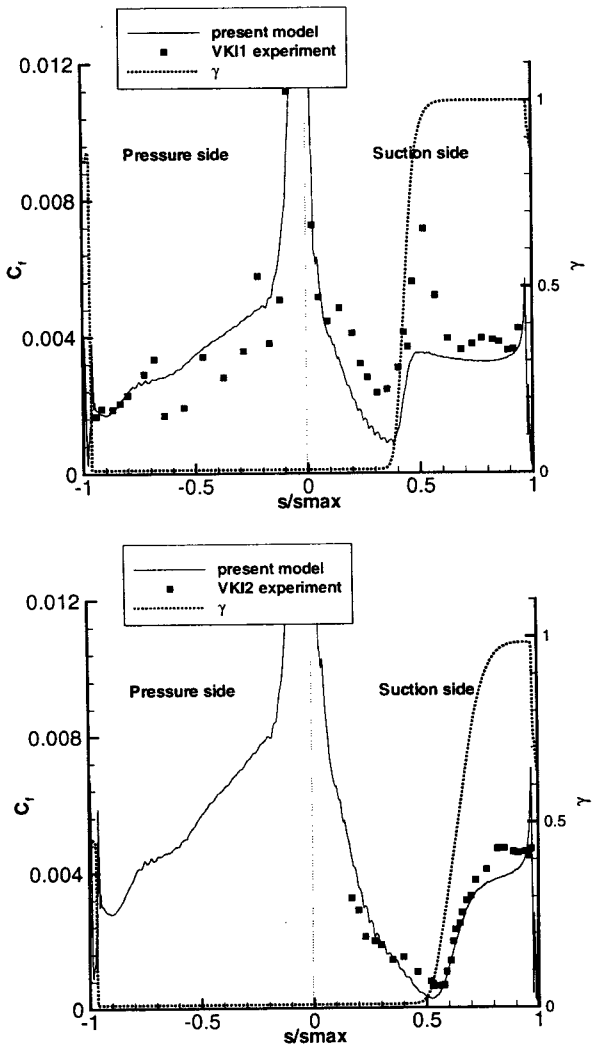

Figure 6: SKIN FRICTION EVOLUTION FOR VKI1 (upper) AND VKI2 (lower) CASCADE.

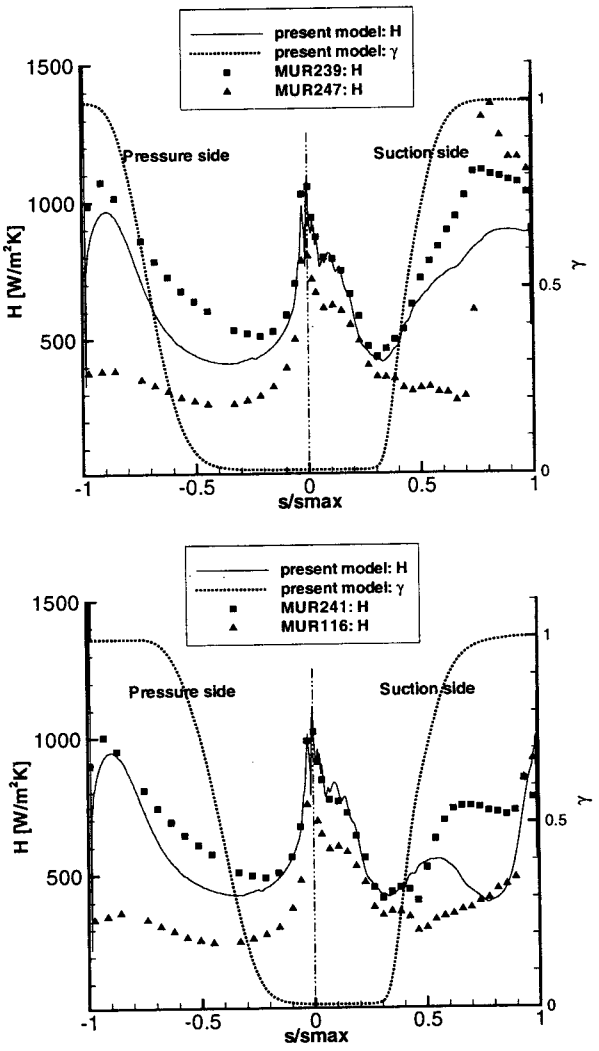

Figure 7: HEAT TRANSFER COEFFICIENT EVOLUTION FOR MUR239 (upper) AND MUR241 (lower) CASCADE. (MUR247 and MUR116 are shown as corresponding cases for low turbulence level.)

Dhawan, S., and Narasimha, R., Some properties of boundary layer during the transition from laminar to turbulent flow motion. *J. Fluid. Mech.*, 3:418–436, 1958.

Kuan, C. L., and Wang., T., Investigation of the intermittent behaviour of transitional boundary layer using a conditional averaging technique. *Int. J. Exp. Heat Transfer, Thermodynamics, and Fluid Mechanics*, 3:157–173, 1990.

Mayle, R. E., The role of laminar-turbulent transition in gas turbine engines. *J. of Turbomachinery*, 113:509–537, 1991.

Medic, G., and Durbin, P. A., Toward improved prediction of heat transfer on turbine blades. *J. of Turbomachinery*, 124:187–192, 2002.

Menter, F. R., Two-equations eddy-viscosity turbulence models for engineering applications. *AIAA J.*, 32:1598–1605, 1994.

Menter, F. R., Esch, T., and Kubacki, S., Transition modelling based on local variables. In W. Rodi and N. Fueyo, editors, *Engineering turbulence modelling and experiments 5*, pages 555–564. Elsevier, 2002.

Savill, A. M., A synthesis of T3 test cases predictions. In O. Pironneau et al., editorsx, *Numerical simulation of unsteady flows and transition to turbulence*, pages 404–442. Proceedings of the ERCOFTAC Workshop held at EPFL 1990, Cambridge University Press, 1992.

Smith, M.C., and Kuethe, A. M., Effects of turbulence on laminar skin friction and heat transfer. *The Physics of Fluid A*, 9:2337–2344, 1966.

Steelant, J., and Dick, E., Modelling of bypass transition with conditioned Navier-Stokes equations coupled to an intermittency transport equation. *Int. J. Num. Methods in Fluids*, 23:193–220, 1996.

Steelant, J., and Dick, E., Modeling of laminar-turbulent transition for high freestream turbulence. *J. Fluids Engineering*, 123:22–30, 2001.

Wilcox, D. C., Simulation of transition with a two equation turbulence model. *AIAA J.*, 32:247–225, 1994.

Yang, Z., and Shih, T. H., New time scale based $k-\varepsilon$ model for near-wall turbulence. *AIAA J.*, 31:1191–1198, 1993.